

An experimental method for validating compressor valve vibration theory

R.A. Habing^{a,*}, M.C.A.M. Peters^b

^a*Department of Mechanical Engineering, University of Twente, P.O. Box 217, Enschede 7500 AE, The Netherlands*

^b*TNO Science and Industry, P.O. Box 155, Delft 2600 AD, The Netherlands*

Received 23 August 2004; accepted 15 March 2006

Abstract

This paper presents an experimental method for validating traditional compressor valve theory for unsteady flow conditions. Traditional valve theory considers the flow force acting on the plate and the flow rate as quasi-steady variables. These variables are related via semi-empirical coefficients which are determined by steady flow experiments. The new experimental methodology permitted the simultaneous measurement of instantaneous valve opening, instantaneous volume-flow rate and instantaneous pressure difference across the valve. Results for an oscillating valve (at 1.9 times the valve resonance frequency) show that the gas force is predicted reasonably accurately. However, the flow rate model should be improved in order to predict the observed hysteresis (30%) and fluctuations in the vena contracta factor.

© 2006 Elsevier Ltd. All rights reserved.

Keywords: Valve oscillation; Two-Microphone method; Vena contracta factor

1. Introduction

Reciprocating compressors are widely used in gas transportation, gas storage and process industries. The compressor can be considered as the heart of an installation and must operate reliably for several years. A worldwide distributed and returned questionnaire identifies the compressor valves as the primary cause (36%) of unscheduled reciprocating compressor shutdowns (Leonard, 1996).

In reciprocating compressors, the piston motion results in periodic increases and decreases in the chamber volume. The entry and exit ports to the chamber are regulated by valves that periodically open and close.

Although structural details may differ considerably, the principle of operation of all types of automatic valves is similar (Touber, 1976). It is possible to distinguish the same basic functional elements in valves of different design (Fig. 1). During discharge, gas is flowing from the high pressure side in the cylinder through the port and separates at the edges of the seat and plate. The plate is pushed against the fixed limiter.

The motion of the valve plate and the unsteady flow of gas through a valve is essentially a fluid-structure interaction problem. Pioneering work in the field of compressor valve modelling has been performed by Costagliola (1950), who

*Corresponding author. Present address: ABB Turbo Systems Ltd., ZXM-1, Bruggerstrasse 71a, 5401 Baden, Switzerland.

E-mail addresses: reinder.a.habing@ch.abb.com (R.A. Habing), rene.peters@tno.nl (M.C.A.M. Peters).

Nomenclature			
A	cross-sectional area of pipe	α	valve flow coefficient
A_p	valve port area	γ	ratio of specific heats
c	speed of sound	δ	measurement uncertainty
c_g	gas force coefficient	Δp	valve flow pressure difference
d_{sr}	sealing rim length	ε	compressibility factor
e_{res}	restitution coefficient	ζ	damping coefficient
F_g	gas force acting on plate	μ	viscosity
h	valve plate displacement	ρ	density
i	imaginary unit	σ	standard deviation
k	wavenumber	Φ_v	valve volume-flow rate
k_s	spring constant	ω	circular frequency
L_g	total edge length	<i>Subscripts and notations</i>	
L_p	valve port length	BVT	basic valve theory
m	effective plate mass	EVT	extended valve theory
M	Mach number of pipe flow	i, j	microphone identification number
p	pressure	max	maximum value
R_1, R_2	plate inner and outer radius	pl	preload
Re	Reynolds number of valve flow	TM	turbine meter
Sh	Shear number of pipe flow	up	upstream position of valve
St	Strouhal number of valve flow	0	undisturbed state
t	time	\pm	before (–) or after (+) collision
T	temperature	$[\cdot \cdot \cdot]$	functional argument
V_{sensor}	sensor output voltage		
x	position		
Y	admittance		

considered a quasi-steady flow around a mass-spring system. The *state of the art* in the field of Computational Fluid Dynamics is the computation of axisymmetric turbulent flow around a circular plate mass-spring system (Matos et al., 2002). Plate impacts and compressibility effects have not been considered. In the field of experimental methods, the unsteady valve opening has often been measured as function of time at constant parameters (piston frequency, mean valve pressure difference, etc.). These measurements have been used to validate linear stability analyses [e.g., Thomann (1978), Böswirth (2000)]. Most of the valve theories that have been employed in the literature [e.g., Costagliola (1950), Linke et al. (1974), Nieter and Singh (1984), Hayashi et al. (1997), Misra et al. (2002)] can be assigned to a single theory which we will refer to it as the Basic Valve Theory (BVT). This theory considers the valve as a *black box* and provides a semi-empirical description of the valve state variables. The state variables are: the instantaneous pressure difference Δp across the valve, the instantaneous volume-flow rate Φ_v through the valve, and the instantaneous valve opening h .

Employing traditional valve theories yields a convenient estimation of the influence of system parameters. For example, the energy consumption of a reciprocating compressor system can be estimated rather quickly, since the mathematical formulation of this system consists of a set of coupled algebraic and ordinary differential equations [e.g., Toubert (1976)]. However, in order to validate the BVT, an experimental method is required which is able to measure accurately and simultaneously the quantities $h(t)$, $\Phi_v(t)$ and $\Delta p(t)$. So far, no such method has been published. Ziada et al. (1986, 1987) elaborated upon the subject of the self-excitation mechanism by measurement of $h(t)$, $\Delta p(t)$ and the mean value of the mass-flow rate. The present paper does not investigate the subject of the self-excitation mechanism, but aims to present a new experimental method (Section 3), which includes measurement of $\Phi_v(t)$, to validate the BVT (Section 2.1). Furthermore, this method is used to discuss the validity of the BVT for unsteady flow conditions (Section 4). At present, it is not known whether the injection of mass by means of the plate motion is responsible for hysteresis effects (van Zon et al., 1990). This paper aims to provide evidence for the hypothesis of Böswirth (2000), which states that two distinct flow regimes are present in the gap between the seat and plate (Fig. 2). In order to address the effects of flow inertia and plate speed to deviations between the experiments and the predictions, we employ the Extended Valve Theory (EVT) (Section 2.2) subsequently.

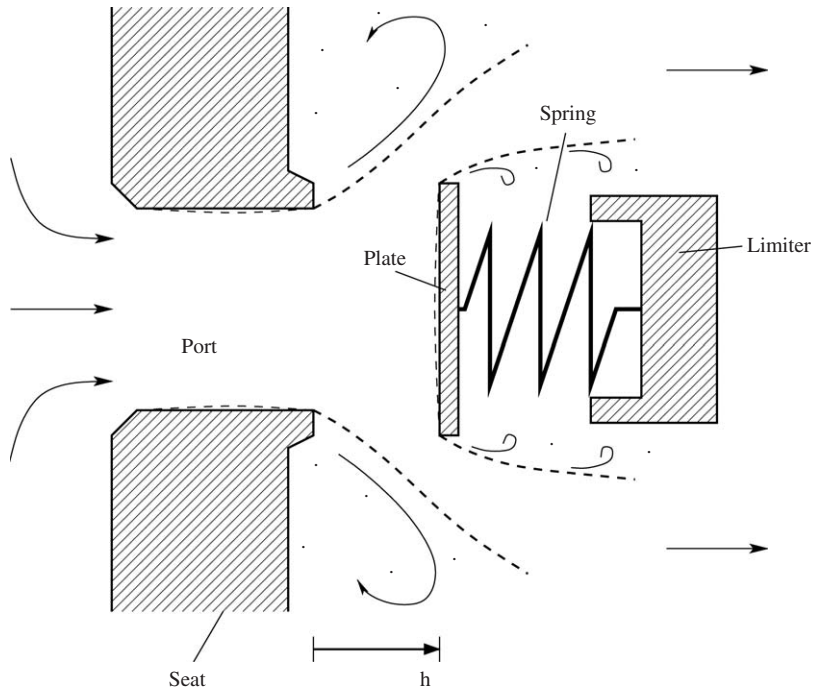


Fig. 1. Sketch of various elements of a compressor valve (h is the valve opening).

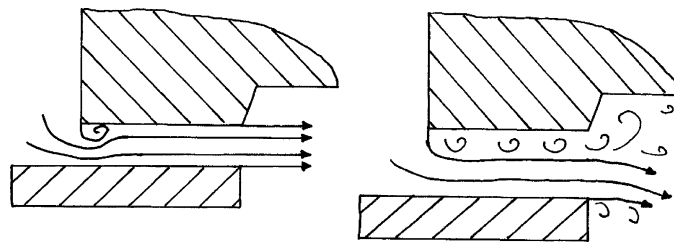


Fig. 2. Flow regimes in a valve during the opening phase. A separation bubble (left) is generated on the seat and becomes longer until a jet (right) is generated. After Böswirth (2000).

2. Valve theory

2.1. Basic valve theory

2.1.1. Fluid dynamics

Consider quasi-steady flow. Then the volume-flow rate Φ_v is expressed as

$$\Phi_v = \alpha \varepsilon L_g h \sqrt{\frac{2}{\rho_{up}} \Delta p}, \quad (1)$$

where L_g is the total edge length of the plate, h is the valve opening (Fig. 1), ρ_{up} is the upstream density and Δp is the pressure difference across the valve. Compressibility effects are accounted for by modifying ε from 1 to $1 - (1/\gamma)(\Delta p/p_{up})$. The effects of viscosity (e.g. vena contracta after flow separation and wall friction) are taken into account by the semi-empirical coefficient $\alpha \sim \mathcal{O}(1)$. This coefficient is found to depend on Reynolds number and geometry; see e.g. Toubert (1976). It is expressed as a functional relation of h . Determination of $\alpha(h)$ is performed by obtaining a (quasi-)steady flow, i.e. a hovering valve plate, and measuring the steady values of h , Φ_v and Δp .

2.1.2. Structure dynamics

The majority of valve models consider the moving parts of a valve as a mass-spring system with a single degree of freedom, i.e.

$$\begin{cases} m \frac{d^2 h}{dt^2} + \zeta \frac{dh}{dt} + k_s(h + h_{pl}) = F_g, & 0 < h < h_{\max}, \\ \frac{dh}{dt}[t_{\pm}] = -e_{\text{res}} \frac{dh}{dt}[t_{\mp}], & h[t_{\pm}] \in \{0, h_{\max}\}, \end{cases} \quad (2)$$

where m is the effective plate mass (Section 4.1), ζ is the damping constant, k_s is the spring constant, h_{pl} is the preload distance and F_g is the gas force acting on the valve plate. Bouncing of the plate with the seat or limiter is modelled with a restitution coefficient e_{res} .

2.1.3. Interaction

The gas force acting on the plate is modelled as the force exerted on the plate in quasi-steady flow, i.e.

$$F_g = c_g A_p \Delta p, \quad (3)$$

where A_p is the port area. The semi-empirical coefficient $c_g \sim \mathcal{O}(1)$ is determined by obtaining a (quasi-)steady flow, i.e. a *hovering* valve plate, and measuring the steady values of h and Δp . This coefficient is expressed as functional relation of h , i.e. $c_g(h)$.

2.1.4. Valve environment

The valve environment determines the type of valve. Common elements are a pipe segment, plenum chamber or an infinitely large reservoir. Self-excited vibration mechanisms are often related to acoustical feedback from the valve environment.

2.2. Extended valve theory

2.2.1. Flow inertia

Unsteady flow in the valve port could modify the phase difference between the pressure difference across the valve and flow rate through the valve, i.e.

$$\Delta p = \frac{1}{2} \rho_{\text{up}} \left(\frac{\Phi_v}{\alpha L_g h} \right)^2 + \rho_{\text{up}} \frac{L_p}{A_p} \frac{d}{dt} \Phi_v, \quad (4)$$

where L_p is the port length.

2.2.2. Plate speed

In case of high velocities of the plate, the outlet flow rate Φ_v^{out} is not equal to the inlet flow rate Φ_v^{in} , even for incompressible flow, i.e.

$$\Phi_v^{\text{out}} = \Phi_v^{\text{in}} - \pi(R_2^2 - R_1^2) \frac{dh}{dt}, \quad (5)$$

where R_1 is the inner radius of the plate and R_2 is the outer radius of the plate.

2.2.3. Laminar flow

Laminar gap flow is expected when the plate is positioned parallel to the seat at very small valve opening ($h < 0.5 d_{sr}$), i.e.

$$\Delta p = \frac{6\mu}{\pi h^3} \left(\frac{d_{sr}}{R_2 - R_1} \right) \Phi_v, \quad (6)$$

where d_{sr} is the sealing rim length and μ is the viscosity.

3. Experimental method

3.1. Design of model valve

Compressor valves have rather complex geometries. Although the present experimental method has been tested successfully on a commercially available compressor valve, considering a simplified valve is more suited for Computational Fluid Dynamics and theoretical modelling. Therefore a model valve has been designed, comprising a less complex geometry while maintaining the essential features of compressor valves (Figs. 3 and 4).

The seat is compatible with a flange, which can be connected to pipe segments (diameter 101.6 mm). During operation, gas flows through the port area and separates at the moving valve part (an aluminium ring plate, Fig. 3, item B). The limiter is connected to the seat by a centrally positioned cylinder. The maximum valve opening is adjustable by an intermediate ring (Fig. 3, item G) between seat and limiter. Quasi-one-dimensional motion of the plate is forced by three guiding rods (separated azimuthally by 120° , Fig. 3, item I and Fig. 4). At the downstream side of the plate, a nylon tube (Fig. 3, item J) is connected to the plate to avoid jamming of plate movement and to force a single degree of freedom (at the expense of additional structural damping, which can be determined empirically). Three preloaded springs are positioned in the limiter holes (separated azimuthally by 120° , Fig. 3, item D). In the centre of every spring, a glassfibre is positioned, mounted on the limiter, to measure the valve opening (Section 3.3). The seat and limiter are constructed from brass, because this material is easy to manufacture, while being strong enough to sustain plate impacts.

3.2. Experimental set-up

In order to measure the three valve quantities h , Φ_v and Δp simultaneously, the following set-up has been realised (Fig. 5). Air is compressed by a centrifugal compressor to a pressure of 8 bar. Steady volumetric flow rates are measured by a turbine flow meter, where corrections for the compressibility of the air are taken into account (Section 3.4). A pressure regulator (CV1) reduces the pressure from 8 bar to atmospheric pressure, thereby preventing pressure pulsations generated downstream from travelling upstream towards the turbine meter. The pulsation source is a rotating cylinder, which blocks the flow periodically. The Two-Microphone method is used to determine the dynamic pressure and dynamic volume-flow rate, just upstream of the model valve (Section 3.5). The steady pressure difference of the valve flow is measured with a strain gauge transducer (Section 3.4). The opening of the model valve is measured with a light intensity method (Section 3.3).

3.3. Valve plate displacement

Early measurements of valve plate displacement have been carried out in the 1930s. The plate was connected to a movable arm carrying a writing stylus. In subsequent decades, many noncontact measurements were performed, e.g. inductive or capacitive transducers (Touber, 1976). However, in general, displacement sensors have several disadvantages, e.g. sensitivity to temperature changes, lack of commercial availability, large physical dimensions relative to the valve system, restriction to dynamic measurements, small spatial resolution, restriction to metallic materials, and inconvenient displacement range.

A rather new class of methods for monitoring the valve opening is the use of optical sensors, like the Laser Doppler Vibrometer method (Buligan et al., 2002), the Endoscope Video method (Ludu et al., 2000), or the Fiber Optic Displacement method (Prasad and Woollatt, 2000).

In the present set-up, three independent glassfibres are connected to the valve limiter (Fig. 3). At every connection, laserlight (wavelength is 820 nm) is reflected at the downstream side of the valve plate. This light is captured by the same fibre and sent to an amplified silicon detector ($0.9 \text{ V}/\mu\text{W}$ at 50Ω). The output is directed to the acquisition system. The intensity of the reflected light is a measure for the distance between plate and fibre, and thus for the valve opening. The aluminium plate surface has a high reflection coefficient for the nearly infrared light. Therefore, on the nonmetallic compressor valve plates, an aluminium layer has to be coated. Calibration takes place by inserting thin shims with well-defined thicknesses ($\delta h < 0.02 \text{ mm}$) between the seat and plate. Every glassfibre has to be calibrated independently, because fibre mountings (laser, limiter and sensor) are set manually. Typical calibration curves are shown in Fig. 6. A common problem of displacement transducers is the offset and range required. At the critical distances, the reciprocal sensitivity increases dramatically, i.e. $dh/dV_{\text{sensor}} \rightarrow \infty$. When the plate is close to the fibre (h is large), an offset phenomenon can be expected because the fibre's end is not a point. When the plate is far away from the fibre (h is

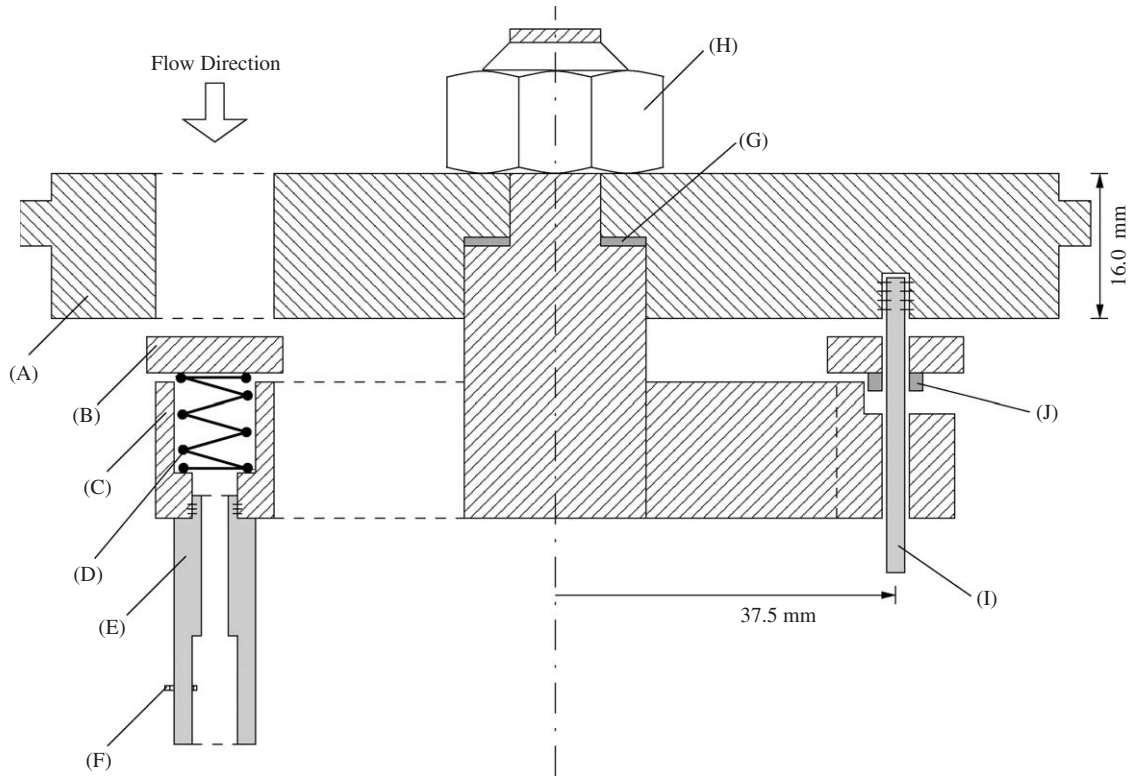


Fig. 3. Model valve assembly (A: seat, B: ring plate, C: limiter, D: spring, E: glass-fibre connector, F: imbus screw to adjust the position of the glassfibre, G: high-tolerance ring to adjust the maximum valve opening, H: locking nut, I: guiding rod, J: nylon tube connected to the plate).

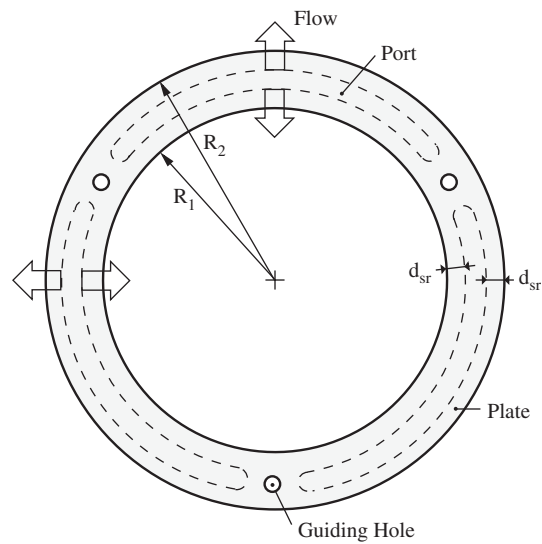


Fig. 4. Sketch of model valve ring plate (R_1 is the inner radius, R_2 is the outer radius, d_{sr} is the sealing rim length).

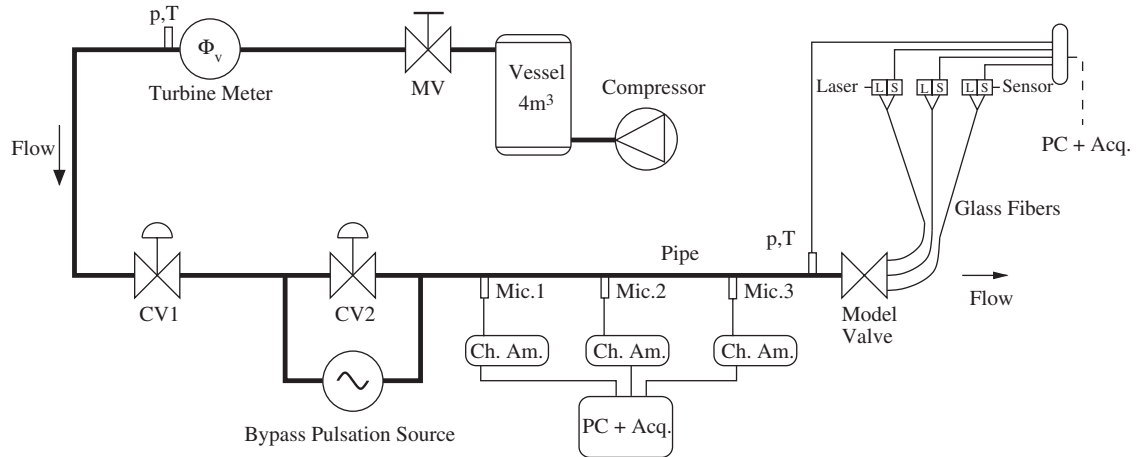


Fig. 5. Experimental set-up (MV = manual valve, CV = control valve, Mic. = microphone, Ch.Am. = charge amplifier, PC + Acq. = personal computer and acquisition interface, L = laser, S = silicon sensor).

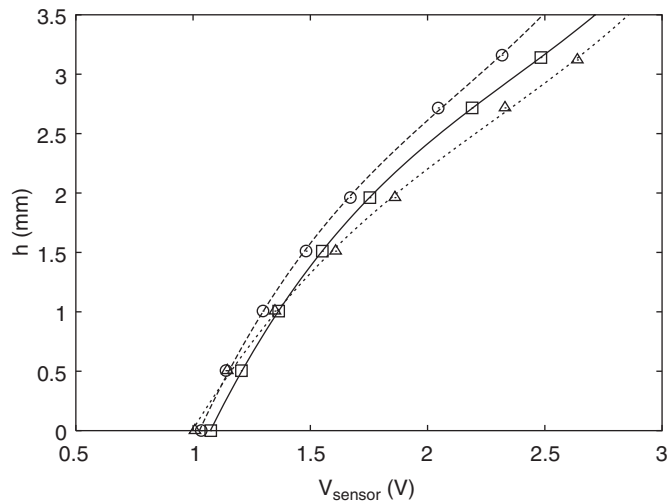


Fig. 6. Valve opening calibration. For every fibre a separate curve is fitted, using a third-order polynomial; $h_{\text{max}} = 3.14$ mm.

small), a weak light intensity is captured. Therefore, a curve fitting of a third-order polynomial is used, which requires at least five data points to obtain a regression coefficient less than unity in general.

A limitation of the method is the detection of the valve plate displacement in the case of a rocking valve plate, i.e. the simultaneous translational and rotational plate motion. Calibration of h is performed for situations in which the plate is parallel to the seat surface. However, the reflected light intensity is a function of the plate tilting angle too. Only for a few angles the calibration can be carried out conveniently. Therefore, quasi-one-dimensional plate motion must be enforced by making use of guiding rods (commercially available compressor valves have guiding rods to prevent plate rotation), at the expense of additional structural damping. The model valve plate is forced to move nearly translationally in which the angle cannot exceed approximately 0.5° . Light intensity measurements for oblique plate positions showed no significant dependence on this angle.

3.4. Static measurements

3.4.1. Valve pressure difference

When the air is flowing (quasi-)steadily through the model valve, a strain gauge transducer determines Δp ($\delta\Delta p = 1 \text{ Pa} + 0.05\%\Delta p$). For conditioning reasons, the ambient pressure is taken as reference. For *steady* pipe flow, the pressure difference between strain gauge and model valve is negligible compared to Δp of the model valve. When an unsteady flow component is superimposed, however, the time-averaged value of Δp is increased due to a nonlinear effect ($\Delta p \sim \Phi_v^2$).

Fig. 7 illustrates the change (8%) in measured mean pressure at the onset of valve oscillation. Before resonance sets in ($t < 70$ s), the valve plate displacement follows the duty cycle of the centrifugal compressor. The steady component of the valve flow pressure difference should be determined from the time-averaged value of Δp during unsteady flow, rather than using Δp at steady flow conditions.

3.4.2. Valve volume-flow rate

The steady flow rate at the location of the turbine meter is determined by measuring the frequency of the generated pulses. In the interval $10\text{--}100 \text{ m}^3/\text{h}$ the measurement error is less than 1%. By assuming one-dimensional steady nonleaking flow of an ideal gas, the valve volume-flow rate is corrected for the drop in density, yielding

$$\Phi_v = \left(\frac{p_{TM}}{p_{up}}\right) \left(\frac{T_{up}}{T_{TM}}\right) \Phi_{v, TM}, \quad (7)$$

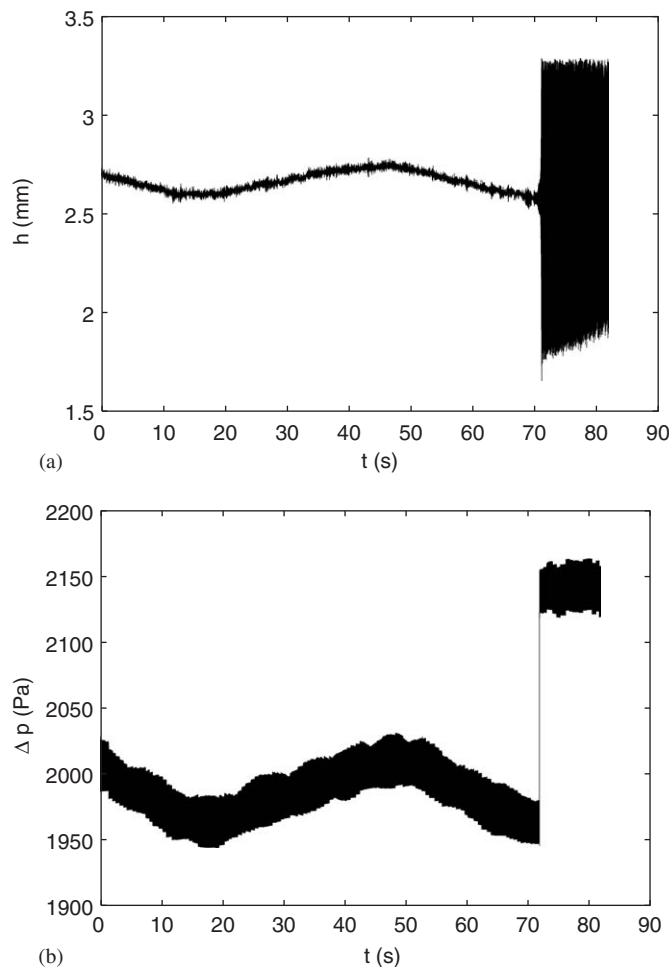


Fig. 7. Increase of time-averaged Δp at onset of unsteady flow. (a) Valve opening; (b) pressure difference.

where the subscript *TM* denotes measurements at the turbine meter and subscript ‘up’ denotes the inlet position of the model valve.

3.5. Dynamic measurements

The unsteady values of Δp and Φ_v are obtained by making use of the linear theory of sound propagation and superposition of dynamic quantities and static quantities. The Two-Microphone method is used to reconstruct the acoustic waves at the inlet of the model valve (Chung and Blaser, 1980a, b, c; Bodén and Åbom, 1986; Åbom and Bodén, 1988). A common procedure is to apply this method in Fourier space (at a single frequency). However, we are interested in time-domain reconstruction, and therefore the method must be extended by using multiple modes. Three piezo-electric transducers (microphones with typical sensitivity of 1400 pC/MPa) are mounted flush at the pipe wall (Fig. 5). A pistonphone is used to calibrate the transducers and charge amplifiers with an accuracy better than 1 Pa. A typical amplitude of the pressure oscillation at the fundamental frequency is 600 Pa.

3.5.1. Two-Microphone method

When the one-dimensional Euler equations are linearised, plane wave solutions for the pressure amplitude and velocity amplitude are obtained. The present flow is a low Mach number flow, which implies identical wavenumbers for upstream- and downstream-travelling waves, i.e. $k = \omega/c$. The experiments are performed at conditions that corrections for (i) Doppler effects and (ii) visco-thermal effects are not necessary, because (a) $M \ll 1$ (typically 1.5×10^{-2}) and (b) $Sh \gg 1$ (typically 2.3×10^2); see, e.g., Peters et al. (1993). Consider the dynamic pressure in Fourier space, i.e. $p(x, \omega) = \int_{-\infty}^{\infty} p(x, t) e^{-i\omega t} dt$. Then the wave reconstruction in the time domain at any position x yields

$$p(x, t) = \frac{1}{2\pi} \int_{-\infty}^{\infty} \frac{p(x_i, \omega) \sin[k(x_j - x)] + p(x_j, \omega) \sin[k(x - x_i)]}{\sin[k(x_j - x_i)]} e^{i\omega t} d\omega, \quad (8)$$

$$\Phi_v(x, t) = \frac{iY}{2\pi} \int_{-\infty}^{\infty} \frac{p(x_j, \omega) \cos[k(x - x_i)] - p(x_i, \omega) \cos[k(x_j - x)]}{\sin[k(x_j - x_i)]} e^{i\omega t} d\omega, \quad (9)$$

where the positions of the two microphones are denoted by x_i and x_j . The admittance $Y = A/\rho_0 c$. Traditionally this method is used for analysis in the frequency domain. Eqs. (8) and (9) contain weight factors as function of $\omega = kc$, yielding convolution integrals for time domain analysis. In evaluation of Φ_v by means of Eq. (1) we will neglect the fluctuations in the density ρ_{up} because $\rho(x, t)/\rho_0 \ll 1$.

3.5.2. Time and frequency filtering

The acquisition interface samples data from the microphones. Therefore, wave reconstruction is performed at a discrete level by using the Fast Fourier Transform. Because this algorithm assumes periodic signals, wrap-around (aliasing) errors are reduced by multiplying the dynamic pressure with the Bingham window. From the three microphone signals, the pair is chosen that has the highest coherence (based on the cross-spectrum and the power spectra).

In order to prevent the introduction of large errors during the reconstruction (Eqs. (8) and (9) can become singular), the frequency filter of Bodén and Åbom (1986) is applied, i.e. $0.1\pi < k|x_j - x_i| < 0.8\pi$. In Fourier space, the remaining modes are zero-padded until the Nyquist frequency. Note that the measured spectrum peaks should be located in this interval, in order to apply the reconstruction method safely. In our case e.g. $|x_j - x_i| = 0.60$ m, yielding $28 \text{ Hz} < \frac{1}{2\pi} \omega < 228 \text{ Hz}$. This interval encloses typical valve resonance frequencies and typical pulsation sources from the by-pass system. However, the valve resonance frequency has not been observed in the spectra. Therefore, the valve oscillation is acoustically driven, in agreement with the experiments of Ziada et al. (1986).

A typical result of the quality of reconstruction is shown in Fig. 8. The acoustic wave is reconstructed from microphones 1 and 2 at the location of microphone 3. This case represents an oscillating valve plate with large amplitude. The issue of modelling a valve as a black box, naturally raises the question of how to define the valve inlet. Reconstruction of the r.m.s. pressure amplitude as a function of x (using Parseval’s identity) reveals that the flow inlet can be defined at the geometrical inlet plane. The valve is an acoustically compact area, i.e. the largest geometrical length scale of the valve is much smaller than the smallest acoustical wave length.

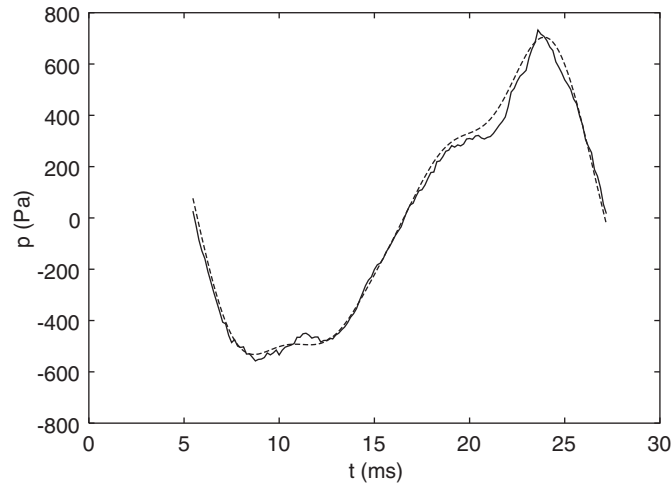


Fig. 8. Dynamic pressure: —, measurement; --, reconstruction.

4. Valve dynamics

4.1. Mechanical valve parameters

The effective plate mass m is obtained by measuring the weight of the plate (including three nylon tubes) and adding the effective spring mass (inertial effect of one coil spring equals one-third of its mass). Consider the valve axis (perpendicular to the seat surface) to be vertically aligned with the gravity vector. The spring constant k_s is then determined by the static spring force $k_s(h + h_{pl})$ balancing the gravity force of added objects of known mass (Fig. 9(a)). The damping coefficient ζ is obtained by generating an underdamped oscillation without flow. The amplitude of h decays exponentially (Fig. 9(b)). The preload distance h_{pl} , total edge length L_g and maximum valve opening h_{max} are obtained by measuring geometrical length scales of valve and springs. The port area A_p is determined from the port length and volume (known from density and mass) of the removed brass after milling. Finally, Table 1 presents the numerical values of the mechanical parameters of the model valve.

4.2. Steady flow

The semi-empirical coefficients are obtained by generating a (quasi-)steady flow. Note that such a flow is a result of fluid-structure interaction, because for a hovering valve plate a unique combination of h , Φ_v and Δp is determined. This (quasi-)steady state is obtained by recognizing six regimes. Consider a fully closed valve and a slowly opening control valve upstream. Then the following regimes will appear subsequently: (i) fully closed valve; (ii) at very small valve openings resonance sets in, the plate is colliding against the seat and later on against the limiter; (iii) fully opened valve. When the control valve upstream is slowly closed, the following regimes will appear subsequently; (iv) (quasi-)steady state; (v) at very small valve openings resonance sets in, the plate is colliding against the seat (slowly opening the control valve yields an irreversible process, i.e. resonance persists); (vi) fully closed valve. In regime (iv), the coefficients $\alpha(h)$ and $c_g(h)$ are determined (see Fig. 10).

In Fig. 10, the valve opening h denotes the averaged value of the three-point measurements. Parabolic regression fits appeared to be adequate from a reproducibility point of view. The standard deviation of $h(t)$ is less than 1% of its mean value. For a ring plate compressor valve, Frenkel (1969) reports α monotonically decreasing from 0.8 to 0.5 and c_g monotonically increasing from 1.0 to 1.3, both for $h/h_{max} \in (0.2, 1.0)$.

4.3. Unsteady flow

4.3.1. Restitution coefficient

The valve plate is limited in its travel by the valve seat and by the limiter. When a moving body impacts a fixed wall it will bounce with a velocity that is generally lower than the velocity before impact. The restitution coefficient, see Eq. (2),

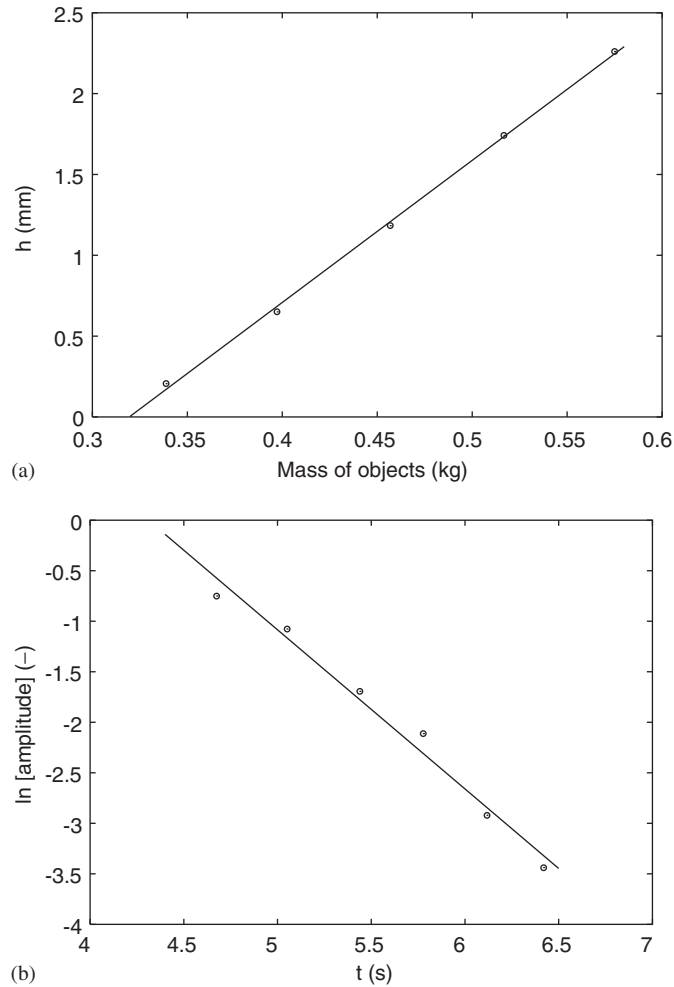


Fig. 9. Determination of mechanical valve parameters. (a) Spring constant k_s (slope $\propto k_s^{-1}$); (b) damping coefficient ζ (ordinate: dimensionless amplitude of h , slope $\propto \zeta$).

Table 1
Mechanical parameters of model valve

Parameter	Symbol	Value
Effective plate mass	m	38.54×10^{-3} kg
Damping coefficient	ζ	1.45 N s/m
Spring constant	k_s	1116 N/m
Preload distance	h_{pl}	3.06 mm
Maximum valve opening	h_{max}	3.14 mm
Port area	A_p	26.61×10^{-4} m ²
Total edge length	L_q	471.2 mm
Port length	L_p	16.00 mm
Inner radius of plate	R_1	30.00 mm
Outer radius of plate	R_2	45.00 mm
Sealing rim length	d_{sr}	1.00 mm

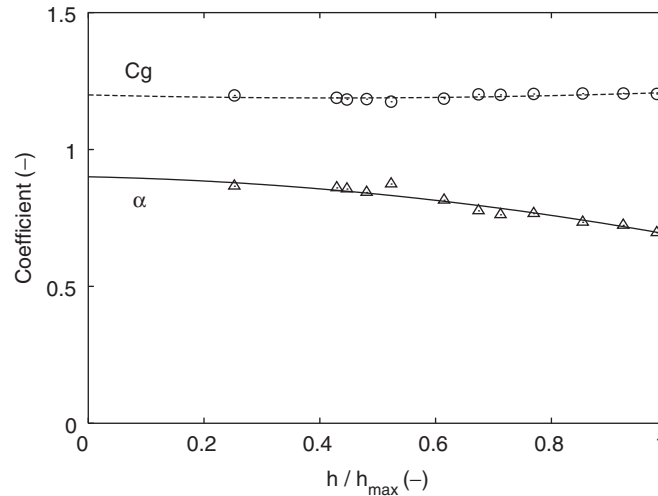


Fig. 10. Semi-empirical coefficients for model valve.

cannot be predicted from the elastic properties of the used materials alone. There are many other (fluid-structure interaction) factors involved. In case of absence of flow, visual observation suggests inelastic ($e_{\text{res}} = 0$) impact. However, online sampling of $h(t)$ reveals that at timescales of $\mathcal{O}(10^{-3} \text{ s})$ and length scales of $\mathcal{O}(10^{-4} \text{ m})$ semi-elastic collisions occur. More specifically, based on multiple rebounds, the model valve has coefficients of restitution of $e_{\text{res}} = 0.2 \pm 0.1$ for the limiter and $e_{\text{res}} = 0.3 \pm 0.1$ for the seat. Similarly to compressor valves, severe rocking effects are only present when the valve plate is close to the seat, in agreement with the Dynamic Stress Concentration Effect hypothesis of Böswirth (2000) to explain valve fracture. We expect that there is an ‘air-cushion’ between the plate and limiter that acts as a fluid damper.

4.3.2. Validation of basic valve theory

The BVT is closed when $\alpha(h)$ and $c_g(h)$ are known. Validation can be performed in several ways. One way is to integrate the equation of motion of the plate, Eq. (2), for prescribed experimentally determined $\Delta p(t)$ and to compare the simulation results for $h(t)$ with the experimentally measured plate height. Fig. 11(a) shows a typical result of the time traces of the three fibre optic transducers. Fig. 11(b) shows that the frequency and phase angle of every mode are in good agreement, while the predicted amplitude is too large. The algebraic flow rate relation, Eq. (1), can be used to compare the *dynamic* flow coefficient (α based on experimentally determined $\Phi_v(t)$, $h(t)$ and $\Delta p(t)$) with the quasi-steady flow coefficient ($\alpha(h)$ based on experimentally determined $h(t)$), see Fig. 11(c). In this case predicting the flow force with the quasi-steady flow assumption yields moderate to good agreement. However, predicting the flow rate through the valve with quasi-steady flow assumption yields large deviations. Fig. 11(d) reveals that hysteretic changes in flow pattern should be taken into account. The hysteresis in the flow coefficient is caused by inertial effects of the flow. However, the Strouhal number¹ $St = \mathcal{O}(10^{-3})$ is very low. We expect this effect to be caused by a periodically detaching ($\alpha \approx 0.7$) and reattaching ($\alpha \approx 1.0$) separated flow from the seat. These two distinct flow regimes are sketched by Böswirth (2000) for the opening phase of a compressor valve, see Fig. 2. The counterclockwise direction of the hysteresis is also reported by van Zon et al. (1990).

In the following analysis, the BVT (Section 2.1) has been extended, referred to as the EVT (Section 2.2), taking into account flow inertia in the valve port, plate speed and laminar gap flow. Laminar flow is expected when the plate is positioned parallel to the seat at very small valve opening ($h < 0.5d_{sr}$). Therefore, extrapolation of the fitted curves for the semi-empirical relations $c_g(h)$ and $\alpha(h)$ (Fig. 10) should be added with data points for $h/h_{\max} < 0.2$. However, steady flow in that region has not been obtained. Employing the extended theory to the conditions of Fig. 11 ($h/d_{sr} > 1.3$ where

¹The Strouhal number is based on the fundamental frequency of the flow rate, sealing rim length and mean valve outlet velocity.

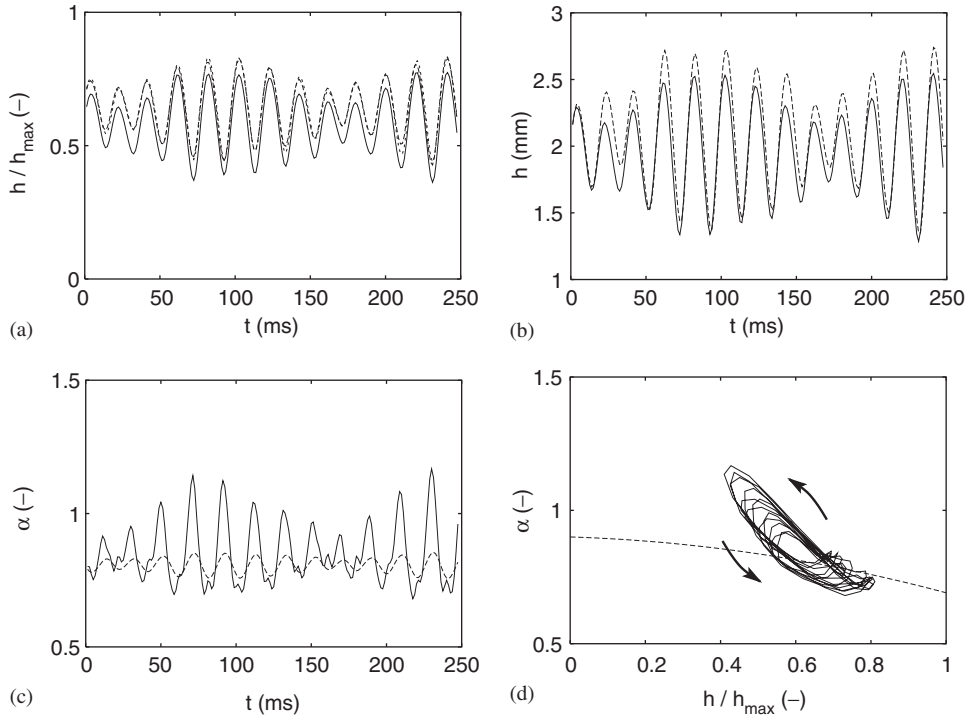


Fig. 11. Validation of Basic Valve Theory. (a) Valve opening measurement of three fibre optic transducers ($h_{\max} = 3.14$ mm); (b) valve opening (—, experiment; --, theory); (c) flow coefficient as function of time (—, experiment; --, theory); (d) flow coefficient as function of valve opening for $t \in (0, 250)$ ms (—, experiment; --, theory). Parameters: $\zeta/m\Omega = 0.12$, $k/m\Omega^2 = 0.29$, $h_{pl}/h_{\max} = 0.97$, $A_p/L_g^2 = 1.20 \times 10^{-2}$, where Ω is the circular frequency of the fundamental mode of pulsation. The sampling frequency is $15.9\Omega/2\pi = 1/\Delta t$.

$d_{sr}/h_{\max} = 0.3$) does not improve the results significantly, i.e.

$$\sigma[h_{\text{BVT}} - h_{\text{EVT}}]/h_{\max} = 1.3 \times 10^{-4},$$

$$\sigma[\Phi_{v,\text{BVT}} - \Phi_{v,\text{EVT}}]/\Phi_{v,\text{mean}} = 6.1 \times 10^{-4},$$

for $t \in (0, 250)$ ms.

5. Concluding remarks

A semi-empirical description of the dynamical response of compressor valves uses the valve opening h , the pressure difference Δp across the valve and the volume-flow rate Φ_v through the valve as basic state variables. The aim of our research is to provide accurate dynamic measurements of these variables.

The experimental method provides next to mean values of Δp and Φ_v (Section 3.4) also measurements of the fluctuations. The analysis is based on an acoustical model and hence cannot be used when shock waves occur (Section 3.5). Furthermore, in the present set-up the tilting angle of the valve plate cannot be larger than 0.5° (Section 3.3). For these conditions, we achieve an accuracy of $\delta h/h_{\max} < 2\%$, $\delta \Delta p/\Delta p_{h_{\max}} < 1\%$ and $\delta \Phi_v/\Phi_{v,h_{\max}} < 2\%$.

Preliminary results for unsteady flow through a simplified valve (Section 3.1) show that the BVT (Section 2.1) is able to predict the gas force acting on the valve plate reasonably accurately (Section 4.3). However, the flow rate through the valve is underpredicted (both mean value and fluctuating parts) at a given pressure difference (Section 4.3). The volume-flow rate during the opening stage is smaller than that during the closing stage, i.e. $\Phi_v[h, \dot{h} > 0] < \Phi_v[h, \dot{h} < 0]$. In our analysis, the BVT has been extended, taking into account flow inertia, plate speed and laminar gap flow (Section 2.2). Results show that the extended model does not describe the fluid-structure interaction processes significantly better than the BVT. Therefore, we expect the flow hysteresis effect of the vena contracta factor α (Fig. 11(d)) to be caused by a

periodically detaching and reattaching flow, separated from the seat. The inertial effects of the flow that are related to this hysteresis effect can be characterised by a new definition of the Strouhal number,² i.e. $St' = \mathcal{O}(1)$.

The fact that our extensions of the BVT do not significantly improve its performance cannot be generalised to actual situations in compressor valves. The range of parameters in valve design (plate mass, spring constant, etc.) has to be further explored before one can generalise our conclusions. In the case of Fig. 11 the Reynolds number³ is in the range of practice, i.e. $Re = 1.7 \times 10^4$. However, the fundamental frequency of the flow is 1.9 times the valve resonance frequency. In reciprocating compressors this ratio could be obtained when the piston (which has a lower frequency than the valve resonance frequency) drives the chamber volume towards its minimum, such that standing waves are generated in the chamber gas.

Acknowledgements

The authors are indebted to A. Hirschberg, J. Bolle and R. Hagmeijer for helpful discussions and to J. van der List for construction of the model valve. This research is financially supported by TNO Science and Industry, Department of Flow and Structural Dynamics (PULSIM).

References

- Åbom, M., Bodén, H., 1988. Error analysis of two-microphone measurements in ducts with flow. *Journal of the Acoustical Society of America* 83, 2429–2438.
- Bodén, H., Åbom, M., 1986. Influence of errors on the two-microphone method for measuring acoustic properties in ducts. *Journal of the Acoustical Society of America* 79, 541–549.
- Böswirth, L., 2000. *Strömung und Ventilplattenbewegung in Kolbenverdichterventilen*. Eigenverlag, Vienna.
- Buligan, G., Paone, N., Revel, G.M., Tomasini, E.P., 2002. Valve lift measurement by optical techniques in compressors. In: *Proceedings of the International Compressor Engineering Conference, Purdue University, USA, Paper C13-5*.
- Chung, J.Y., Blaser, D.A., 1980a. Transfer function method of measuring in-duct acoustic properties: I Theory. *Journal of the Acoustical Society of America* 68, 907–913.
- Chung, J.Y., Blaser, D.A., 1980b. Transfer function method of measuring in-duct acoustic properties: II Experiment. *Journal of the Acoustical Society of America* 68, 914–921.
- Chung, J.Y., Blaser, D.A., 1980c. Transfer function method of measuring acoustic intensity in a duct system with flow. *Journal of the Acoustical Society of America* 68, 1570–1577.
- Costagliola, M., 1950. The theory of spring-loaded valves for reciprocating compressors. *Journal of Applied Mechanics* 17, 415–420.
- Frenkel, M.I., 1969. *Kolbenverdichter: Theorie, Konstruktion und Projektierung*. VEB Verlag Technik, Berlin.
- Hayashi, S., Hayase, T., Kurahashi, T., 1997. Chaos in a hydraulic control valve. *Journal of Fluids and Structures* 11, 693–716.
- Leonard, S.M., 1996. Increase reliability of reciprocating hydrogen compressors. *Hydrocarbon Processing*, January, 67–74.
- Linke, A., Fischer, M., Göldner, H., 1974. Komplexrechenprogramm zur Optimierung und Simulation des Arbeitsprozeßablaufs und des Ventilverhaltens von Hubkolbenverdichtern. *Luft- und Kältetechnik* 10, 302–306.
- Ludu, A., Betto, A., Regner, G., 2000. Endoscope video of compressor valve motion and pressure measurement assist simulations for design improvements. In: *Proceedings of the International Compressor Engineering Conference, Purdue University, USA*, pp. 443–450.
- Matos, F.F.S., Prata, A.T., Deschamps, C.J., 2002. Numerical simulation of the dynamics of reed type valves. In: *Proceedings of the International Compressor Engineering Conference, Purdue University, USA, Paper C15-2*.
- Misra, A., Behdian, K., Gleghorn, W.L., 2002. Self-excited vibration of a control valve due to fluid-structure interaction. *Journal of Fluids and Structures* 16, 649–665.
- Nieter, J.J., Singh, R., 1984. A computer simulation study of compressor tuning phenomena. *Journal of Sound and Vibration* 97, 475–488.
- Peters, M.C.A.M., Hirschberg, A., Reijnen, A.J., Wijnands, A.P.J., 1993. Damping and reflection coefficient measurements for an open pipe at low Mach and low Helmholtz numbers. *Journal of Fluid Mechanics* 256, 499–534.
- Prasad, B.G.S., Woollatt, D., 2000. Valve dynamic measurements in a VIP compressor. In: *Proceedings of the International Compressor Engineering Conference, Purdue University, USA*, pp. 361–368.
- Thomann, H., 1978. Oscillations of a simple valve connected to a pipe: part II Experiments. *Journal of Applied Mathematics and Physics* 29, 75–84.
- Touber, S., 1976. A contribution to the improvement of compressor valve design. Ph.D. Thesis, Delft University, The Netherlands.

²This Strouhal number is based on the fundamental frequency of the flow rate, mean valve opening and maximum plate velocity.

³The Reynolds number is based on the mean flow speed in the port, port length and viscosity of air.

- van Zon, J., Hirschberg, A., Gilbert, J., Wijnands, A., 1990. Flow through the reed channel of a single reed music instrument. In: *Supplément au Journal de Physique, Colloque de Physique C2*, vol. 51, pp. 821–824.
- Ziada, S., Shine, S.J., Bühlmann, E.T., 1986. Self-excited vibrations of reciprocating compressor plate valves. In: *Proceedings of the International Compressor Engineering Conference*, Purdue University, USA, pp. 398–414.
- Ziada, S., Shine, S.J., Bühlmann, E.T., 1987. Tests on the flutter of a multi-ring plate valve. In: *Proceedings of the International Conference on Flow Induced Vibrations*, BHRA, pp. 393–401.